Electron attachment to the perfluoroalkanes n-C_NF_{2N+2} ($N = 1$–6) using high pressure swarm techniques[a)]

S. R. Hunter[b)] and L. G. Christophorou[b)]
Atomic, Molecular and High Voltage Physics Group, Health and Safety Research Division, Oak Ridge National Laboratory, Oak Ridge, Tennessee 37830

(Received 8 August 1983; accepted 6 March 1984)

The electron attachment rate constants and negative ion formation mechanisms for six perfluoroalkanes [n-C_NF_{2N+2} ($N = 1$–6)] have been studied in a high pressure swarm experiment within the mean electron energy range from thermal energy ($\approx$0.04 eV) to $\approx$4.9 eV. These experiments were performed over a total gas number density range of 3.2×10^{19} to 3.9×10^{20} cm^{-3} using N_2 and argon as buffer gases. Dissociative electron attachment was found to be the only negative ion formation process for CF_4 and C_2F_6. For C_3F_8, n-C_4F_{10}, and n-C_5F_{12} the electron attachment rate constant measurements exhibited a large total pressure dependence which was strongest for C_3F_8 and decreased with increasing size of the perfluoroalkane molecule. These measurements have been interpreted as electron attachment by parent negative ion formation due to three-body stabilization processes of the initially excited, short-lived (5×10^{-11} s $< \tau < 10^{-8}$ s) parent anion. The lifetimes of these transient parent anions have been found to depend on the nature of the parent ion and on the electron energy. The electron attachment rate constants are largest for the n-C_6F_{14} molecule and decrease with decreasing size of the perfluoroalkane molecule. Furthermore, the peak in the attachment rate constants occurs at the lowest mean energy ($\sim$1.1 eV) for n-C_6F_{14} and shifts to higher mean energy with decreasing size of the molecule (to $\geqslant$5 eV for CF_4). The electron attachment cross sections for all of these molecules have been calculated using the swarm-unfolding method and calculated electron energy distribution functions in argon. These measurements are compared with relative negative ion cross sections, determined previously using mass spectrometric techniques. The negative ion formation mechanisms are discussed and the effect of molecular size on the electron attachment properties of these molecules is indicated using the present measurements in conjuction with the results of a recent single collision negative ion study.

I. INTRODUCTION

An increasing number of uses have been found in recent years for the lower-order perfluoroalkanes (C_NF_{2N+2}, where $N = 1$–6) in a wide variety of applications (e.g., fast gas mixtures for neutron counters,[1] diffuse-discharge opening switch mixtures,[2] unitary and binary gas mixtures for high voltage gaseous[3–5] and liquid[6] insulants) due primarily to their large and desirable energy dependent electron attachment rate constants k_a. (The four gases CF_4 to n-C_4F_{10} have the further desirable characteristics of being chemically and thermally stable, nontoxic, and having high vapor pressures.[7]) The study of the electron attaching properties of these molecules is also of considerable theoretical interest. The present swarm studies provide information on the negative ion formation and decay channels, and on the position and magnitude of the negative ion resonances of these molecules.

Dissociative electron attachment processes are the only mechanisms of negative ion formation observed in CF_4 and C_2F_6, whereas parent negative ion stabilization is the predominant negative ion formation process for C_3F_8 to n-C_6F_{14} at the total gas pressures used in these experiments. These effects are discussed in detail later in this paper. This work was performed in conjuction with a single collision beam experiment using a time-of-flight mass spectrometer[8] (hereafter called paper I), in which the parent and fragment negative ions produced by low-energy electron impact have been observed. The total negative ion yields for CF_4 and C_2F_6 from that study have been normalized to the total attachment cross section σ_a derived from the present swarm data. The energy dependences of σ_a from both studies have also been compared for all six of the perfluoroalkanes.

II. EXPERIMENTAL

A. Method

The technique used to obtain the electron attachment rate constants in the present swarm studies was originally devised by Bortner and Hurst[9,10] to study electron attachment processes in O_2/Ar gas mixtures. More recently, the technique has been used to study the electron attaching properties of several chlorinated and fluorinated hydrocarbons which have possible uses as high voltage gaseous insulants.[11]

In Fig. 1 is shown the schematic diagram of the present apparatus. Electrons are produced in a plane at the source electrode, perpendicular to the applied electric field E by the passage through the gas of high energy alpha particles. The alpha particle trajectories are well collimated such that the

[a)] Research sponsored by the Department of Electric Energy Systems and the Office of Health and Environmental Research, U. S. Department of Energy, under contract W-7405-eng-26 with the Union Carbide Corporation.

[b)] Also, Department of Physics, The University of Tennessee, Knoxville, Tennessee 37996.

 0021-9606/84/126150-15$02.10

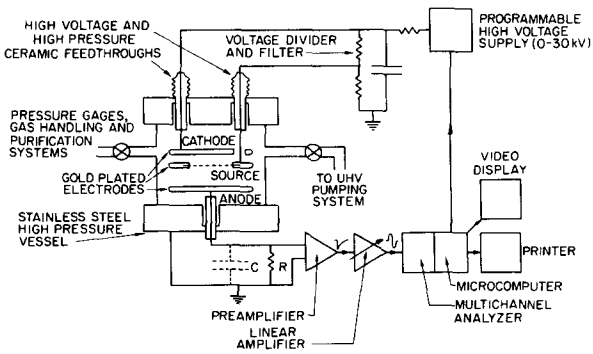

FIG. 1. Schematic diagram of the electron attachment apparatus and signal conditioning electronics used for the present measurements.

electron swarms produced by the energy decay of the alpha particles lie in a well-defined plane at the source. Each alpha particle (produced by the decay of Cf^{252}, energy ≈ 6.1 MeV) produces a swarm of $\approx 2.3\times10^5$ e in Ar and $\approx 1.7\times10^5$ e in N_2 within $\approx 5\times10^{-9}$ s at 133 kPa to $\sim 2\times10^{-10}$ s at 3.2 MPa (Ref. 12). These swarms of electrons then drift to the anode under the influence of a uniform electric field established between the cathode and anode.

When the time constant of the anode circuit $\tau_A = RC$ is large compared with the transit time of the electron swarm, $\tau_1(\tau_A \approx 10^{-3}$ s and $\tau_1 \approx 10^{-6}$–10^{-5} s in these experiments), the voltage pulse from the linear amplifier is[9]

$$V(\tau) = \frac{A\exp[-\tau/\tau_0]}{(\tau_1 - \tau_0 f)} \times\left[(\exp(U\tau_1)-1)\tau - \exp(U\tau_1)(\tau_1 - 1/U) - \frac{1}{U}\right], \quad (1)$$

where $A = n_0 e/C$, $f = (\eta/N_a)N_a d$, $U = (\tau_1 - \tau_0 f)/\tau_0\tau_1$, n_0 is the initial number of electrons produced by *each* α particle at the beginning of the drift space, e is the electronic charge, C is the effective capacitance to ground at the anode and includes contributions from the capacitance between the electrodes, the input of the preamplifier and connecting cables (≈ 50 pF), η/N_a is the attachment coefficient in units of cm^2, N_a is the partial attaching gas number density, d is the drift distance between the source electrode and the anode, and τ_0 is the linear amplifier differentiating and integrating time constant[9] ($\tau_0 = 15$ μs in these experiments).

The maximum in the voltage pulse out of the linear amplifier at time τ', $V(\tau')$ can be found from

$$\frac{dV(\tau')}{d\tau} = 0. \quad (2)$$

Thus,

$$\tau' = \frac{\exp[U\tau_0][\tau_0 + \tau_1 - 1/U] + [1/U - \tau_0]}{[\exp[U\tau_0] - 1]}. \quad (3)$$

Equation (3) is then substituted into Eq. (1) to find $V(\tau')$. The time constant of the amplifier τ_0 is such that over the E/N (electric field strength to total gas number density) range of these experiments in both N_2 and Ar, it falls within the following range of τ_1: $0.5\,\tau_1 < \tau_0 < 10\,\tau_1$. Since the drift velocity of the negative ions in this study is ~ 1000 times less than that of the electrons at a given E/N, it is assumed that the linear amplifier does not respond to any slowly time varying voltages that would be induced on the anode by the motion of the ions in the drift gap. The measurements were performed at high total gas pressures (133 kPa $\leqslant P_T \leqslant$ 3.9 MPa) such that the influence of diffusion upon the drift of the electron swarm was negligible.

To obtain the attachment coefficients, the experiment is performed as follows: A pure buffer gas sample is admitted into the vessel at a given pressure and a distribution of voltage pulse heights are obtained at a given E/N, which are accumulated in a multichannel analyzer (MCA) operating in the pulse height analysis mode. The most probable pulse height is recorded. The E/N is changed and a series of most probable pulse heights is obtained as a function of E/N. If the pressure dependence of the attachment process is to be studied, then the above set of measurements are performed over a range of buffer gas pressures as well. A small quantity of attaching gas is then added to the drift vessel (usually one part in 10^5–10^8 of the total gas pressure in the present study), the chamber refilled with the buffer gas, and a new series of most probable pulse heights obtained as a function of E/N and P_T. The ratio of the pulse heights with and without the attaching gas is obtained. The maximum voltage from the amplifier is obtained when no electron attaching processes are present, thus

$$V(\tau') = A\exp[-1]. \quad (4)$$

Consequently, from the pulse height ratios and Eq. (4), the voltage obtained with the attaching gas added can be found. The attachment coefficient is then obtained by an iterative procedure using Eqs. (1) and (3) to find f and hence (η/N_a).

The partial pressure of the attaching gas is extremely small, and thus it is permissible to assume that the influence of the attaching gas on the electron energy distribution function is negligible. Any influence that is present can be observed by performing the measurements as a function of the partial attaching gas pressure, and the resultant pressure independent attachment rate constants can be obtained from an extrapolation of the rate constants to zero partial attaching gas pressure. Thus, the drift velocity of the swarm is assumed to be that of the pure gas which can be measured in a separate experiment. The transit time $\tau_1 = d/w$ (where w is the electron swarm drift velocity) and the measured attachment rate constant $k_a = \eta w/N_a$ can then be obtained as a function of E/N. The drift velocity measurements of Lowke[13] and Robertson[14] obtained at low gas pressures ($P_T < 100$ kPa) in N_2 and Ar, respectively, were used in these studies. At the higher gas pressures used in the experiments ($P_T > 500$ kPa) multiple scattering processes can modify the electron drift velocity, and hence the apparent k_a, particularly at electron energies near thermal energies.[15] The electron drift velocities in N_2 were corrected using the measurements of Grünberg.[16] Bartels[17] has also observed pressure dependent drift velocities in Ar near thermal energy, but since the lowest mean electron energy used in the present studies in Ar was 0.3 eV, corrections to the high pressure drift velocities are negligible. The measured gas pressures were corrected for compressibility at the higher gas pressures.[18] These effects introduce a 1–2% uncertainty in the measurements at high gas pressures and low E/N values.

TABLE I. Sources of errors and their estimated uncertainties in the swarm electron attachment apparatus.

Source	Error
Drift distance	± 0.5%
Chamber temperature	± 0.3%
Total gas pressure	± 0.5%
Electric field voltage	± 0.2%
Partial attaching gas pressure	± 2.0%
Electron swarm transit time	± 0.5%
Statistical uncertainty in determining the average electron signal pulse height	± 0.5%–2%
Approximations in the analysis of the pulse heights to obtain the electron attachment rate constants	Expected to be small when the electron swarm transit time ≤the time constant of the linear amplifier (15 μs)
Nonideal response characteristics of the linear amplifier	The same conditions apply as above

B. Apparatus

The experimental apparatus is shown schematically in Fig. 1. The drift region electrodes are housed in a stainless steel high pressure vessel, capable of operating at total gas pressures up to 10 MPa. The chamber is pumped by a UHV pumping system with a base pressure of a few parts in 10^{-6} Pa and an outgassing rate of 10^{-3} Pa per h. All electrodes in the chamber are gold plated and enameled insulators are used to reduce possible surface reactions with reactive attaching gases. The alpha particle source used in these studies was Cf^{252} which was electroplated onto a thin platinum ribbon and housed within the source electrode. This source produced $\approx 10^4$ detectable swarms per s. The induced anode voltages, produced by the motion of the swarm, are detected and amplified by a preamplifier and linear amplifier and passed into a microprocessor based, 2048 channel multichannel analyzer (MCA), where the distribution of the resultant peak pulse heights are stored. The pulse height histogram is analyzed by the microprocessor to find the most probable pulse height, which is then used to obtain η/N_a, and thus k_a using a simple numerical iterative procedure. The microprocessor then resets the programmable voltage supply and hence the E/N value, and a new histogram is obtained, and the whole procedure repeated.

An analysis of the experimental errors using this procedure is given in Table I. The total uncertainty in these experiments is estimated to be 5%–7%, which is approximately half that reported previously using this procedure.[11] The major improvements in the apparatus which have led to the reduced uncertainty are in the procurement of higher performance pressure gauges, a considerably stronger α-particle source, and numerical averaging of the pulse height histograms which has led to a statistical uncertainty in the peak voltage of ± 0.5% to 2.0%.

C. Gas purity

The electron attachment measurements were performed using both N_2 and Ar as buffer gases in order to cover the mean electron energy range from near-thermal energy (≈0.04 eV) to ≈4.9 eV. Matheson ultrahigh purity N_2 (99.999%) and Matheson grade Ar (99.9995%) were used in these studies. Both gases were subjected to liquid nitrogen temperatures for ~15 h before use in order to freeze out condensible impurities (e.g., water vapor) which could affect the voltage pulse heights. The vapor from each of these gases was then extracted at temperatures just above the boiling point for each gas. It was necessary to use this procedure as it was found that the minute traces of impurities in the buffer gases could have a measurable effect on the voltage pulse heights. This procedure gave stable pulse height measurements which were reproducible to within ± 5 channels in 2000 during the course of these measurements.

The gases CF_4 and C_2F_6 were obtained from Matheson Gas Products with a stated purity of 99.6%, C_3F_8 from Union Carbide Corporation, Linde Division, with a stated purity of 99%, n-C_4F_{10} and n-C_5F_{12} from Columbia Organic Chemicals Company with a stated purity of 95%, and n-C_6F_{14} from Pierce Chemical Company with a stated purity of >95%. These gases were subjected to gas chromatography (GC) and positive ion mass spectrometric analysis, as well as the negative ion studies of paper I.[8] From these studies, it is estimated that all of these perfluoroalkanes, except possibly n-C_4F_{10} and n-C_5F_{12}, were at least 99.9% pure. The negative ion studies detailed in paper I indicated that the n-C_4F_{10} sample may have been contaminated with up to 5% of the isomer iso-C_4F_{10}. The GC study, which had a detection threshold of greater than 0.1%, failed to detect any isomers in this sample. These apparently contradictory results have not been resolved. Indirect evidence was also found in the negative ion studies reported in paper I that the n-C_5F_{12} sample may have contained up to 5% of c-C_5F_{10}. The influence of this impurity on the measured electron attachment rate constants is discussed in Sec. V. These gases and liquids were subjected to several vacuum distillation cycles prior to any measurements in order to remove air from the samples.

III. RESULTS

The attachment processes observed in the present study for the perfluoroalkanes can be explained by the following reaction scheme:

$$\mathrm{PFA} + \mathrm{e} \xrightarrow{k_1} \mathrm{PFA}^{-*} \begin{cases} \xrightarrow{\nu_2,\ \tau_a} e' + \mathrm{PFA}, & (5a) \\ \xrightarrow[M]{k_3} \mathrm{PFA}^- + \text{energy}, & (5b) \\ \xrightarrow{k_4} C_x F_y^- + C_{N-x}F_{2N+2-y}, & (5c) \end{cases}$$

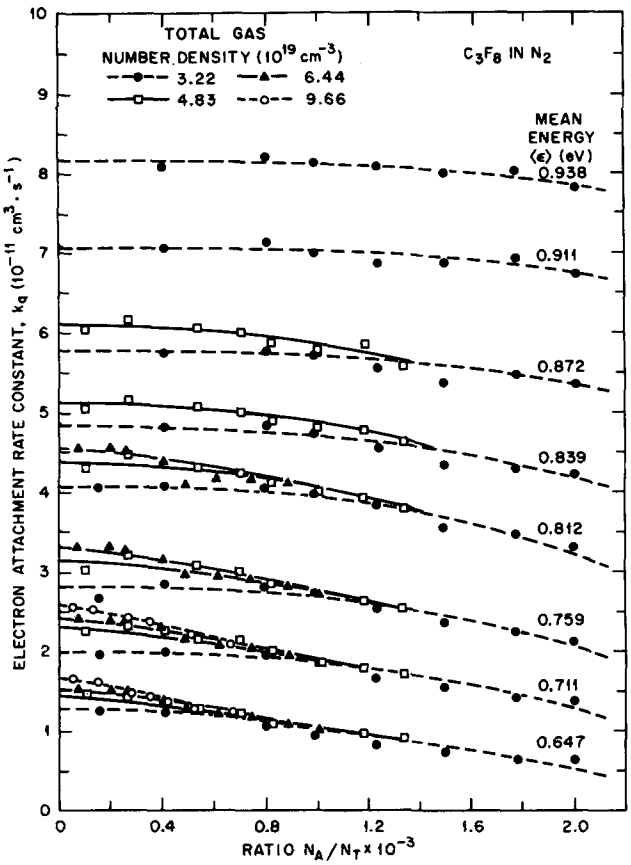

FIG. 2. Electron attachment rate constant k_a for C_3F_8 as a function of the ratio of the attaching gas number density N_A to the total gas number density N_T for four total gas pressures and several values of the mean electron energy.

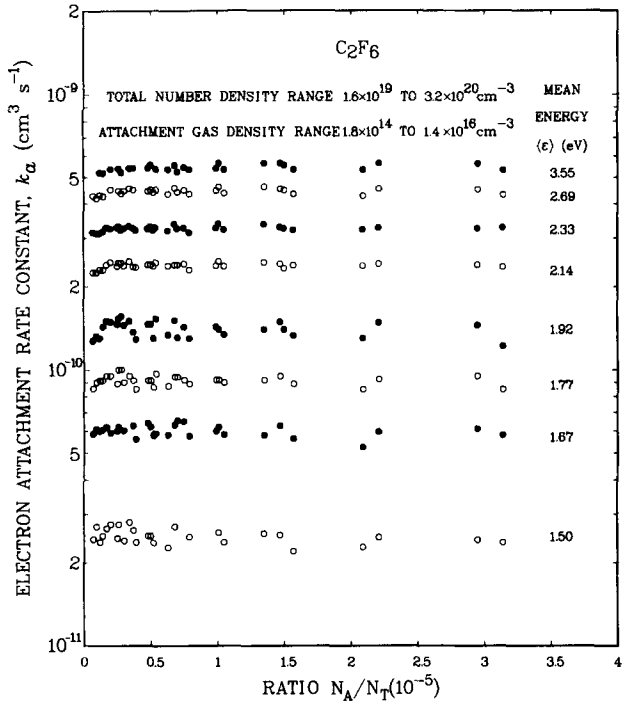

FIG. 3. The electron attachment rate constant k_a for C_2F_6 as a function of the ratio of the attaching gas number density N_A to the total gas number density N_T over the range of N_A, N_T, and $\langle\epsilon\rangle$ shown in the figure.

where the values of x and y depend on the size of the parent molecule.[8] An electron is initially captured by the PFA molecule with an electron attachment rate constant k_1 to form a temporary parent negative ion. This ion can then either autoionize with a decay constant ν_2 and characteristic lifetime τ_a, be collisionally stabilized by another molecule M (usually a buffer gas molecule in these experiments), with a rate constant k_3 to form a stable parent negative ion, or fragment to form negative ions and neutral fragments of the parent molecule with a rate constant k_4. In the absence of process (5c) competition between decay channels (5a) and (5b) lead to a dependence of the measured attachment rate constant k_a on the total gas pressure (or total number density N_T).

The electron attachment rate constants for the perfluoroalkanes were measured at room temperature ($T\approx300$ K) in buffer gases of N_2 over the mean electron energy range 0.04–0.957 eV and in Ar over the mean electron energy range 0.30–4.89 eV (the method for calculating the $\langle\epsilon\rangle$ values is outlined in Sec. IV B.) Between eight and 12 independent sets of measurements were performed in both buffer gases over a wide range of total gas pressures (0.133–3.9 MPa) and partial attaching gas pressures. Two examples of the resultant k_a as a function of attaching gas number density N_a to total number density N_T ratio for several values of $\langle\epsilon\rangle$, are shown in Figs. 2 and 3 for C_3F_8 in N_2 and C_2F_6 in Ar, respectively. Whenever a dependence of k_a on N_a was observed (as in the C_3F_8/N_2 mixture, for example), the measurements were extrapolated to zero N_a to obtain the pressure independent values of k_a. The values of k_a for C_3F_8, n-C_4F_{10}, and n-C_5F_{12} are dependent on the total gas pressure in Ar, while only the k_a for C_3F_8 is pressure dependent in N_2, as can be seen from the measurements shown in Fig. 2. The measurements of k_a in C_3F_8, n-C_4F_{10}, and n-C_5F_{12} in Ar are shown in Figs. 4–6, respectively.

The rate equations for the three-body stabilization process are

$$\frac{dn_e(t)}{dt} = -\nu_1 n_e + \nu_2[\mathrm{PFA}^{-*}] \tag{6}$$

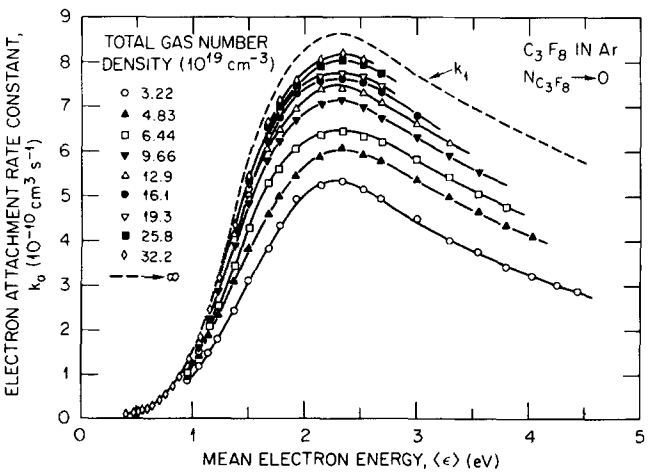

FIG. 4. The electron attachment rate constant k_a for C_3F_8 measured as a function of mean electron energy $\langle\epsilon\rangle$ and total gas number density N_T in a buffer gas of argon. The values of k_a have been obtained by extrapolating the measured k_a to zero C_3F_8 number density N_A.

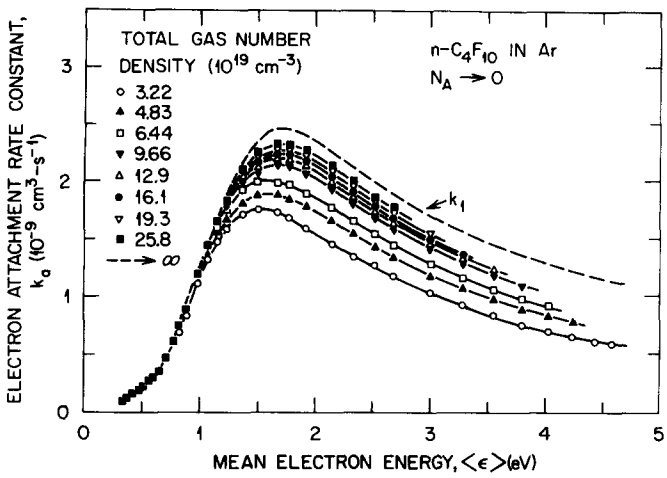

FIG. 5. The electron attachment rate constant k_a for n-C_4F_{10} measured as a function of mean electron energy $\langle\epsilon\rangle$ and total gas number density N_T in a buffer gas of argon.

and

$$\frac{d[\mathrm{PFA}^{-*}](t)}{dt} = \nu_1 n_e - (\nu_3 + \nu_2)[\mathrm{PFA}^{-*}], \qquad (7)$$

where n_e is the electron number density, $[\mathrm{PFA}^{-*}]$ is the number density of the transient parent negative ions, and ν_1 to ν_3 are the collision frequencies in units of s^{-1} for the rate constants k_1 to k_3. They are related by $\nu_1 = k_1 N_a$, $\nu_2 = 1/\tau_a$, and $\nu_3 = k_3 N_T$, where N_a is the number density of the attaching gas. Eliminating $[\mathrm{PFA}^{-*}]$ from Eqs. (6) and (7) gives the following rate equation:

$$\frac{d^2 n_e}{dt^2} + (\nu_1 + \nu_2 + \nu_3)\frac{dn_e}{dt} + \nu_1\nu_3 n_e = 0. \qquad (8)$$

This equation may be solved to find the observed electron attaching collision frequency $\nu_{\mathrm{att}} = 1/\tau_{\mathrm{att}}$, where τ_{att} is the mean time between attaching collisions, from the following

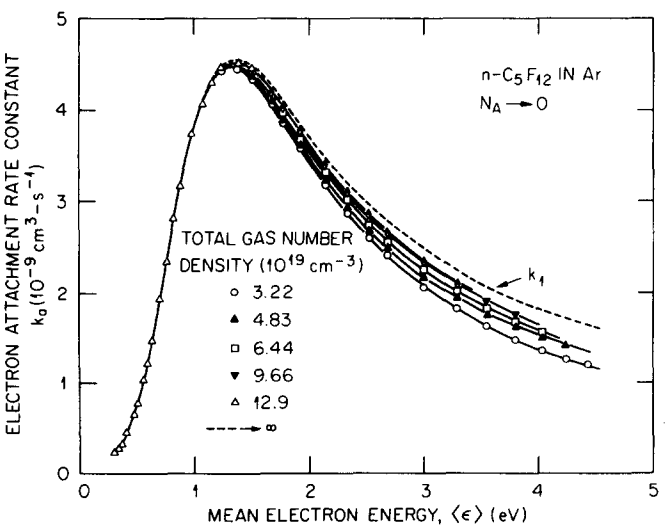

FIG. 6. The electron attachment rate constant k_a for n-C_5F_{12} measured as a function of mean electron energy $\langle\epsilon\rangle$ and total gas number density N_T in a buffer gas of argon.

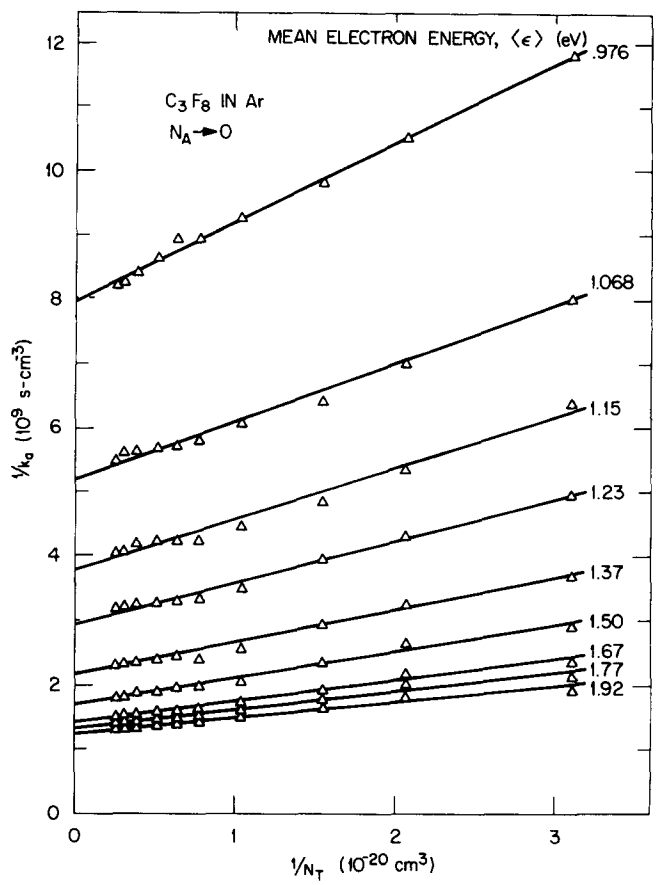

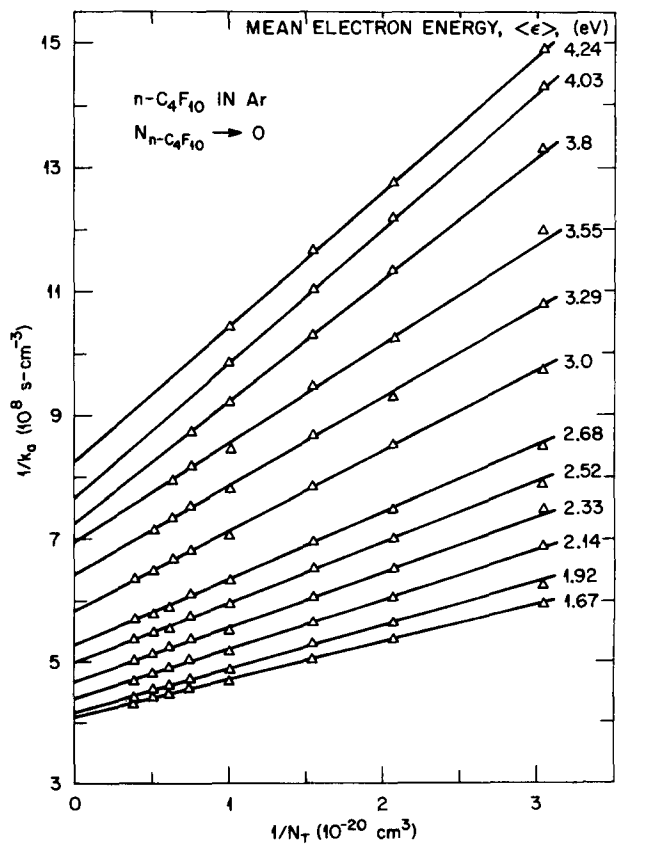

FIG. 7. The inverse of the electron attachment rate constant k_a plotted as a function of the inverse of the total gas number density N_T for several mean electron energies $\langle\epsilon\rangle$ in argon for (a) C_3F_8 and (b) n-C_4F_{10}.

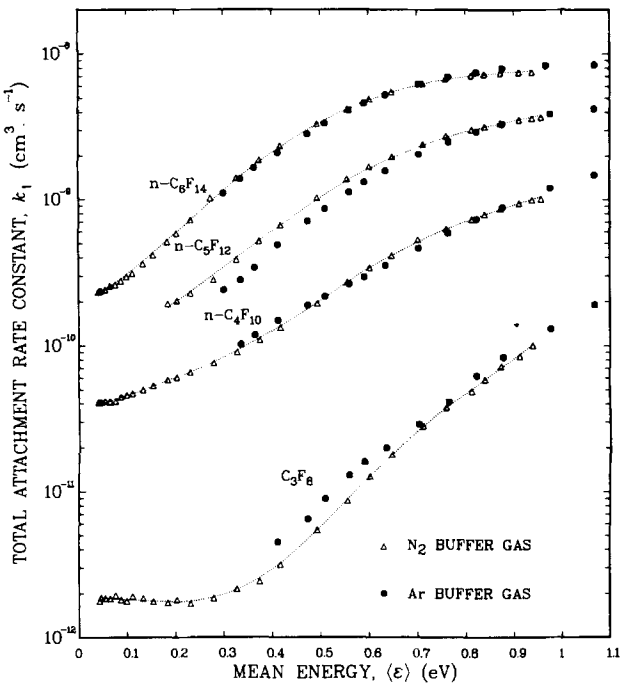

FIG. 8. Electron attachment rate constants k_1 for the perfluoroalkanes measured as a function of mean electron energy $\langle\epsilon\rangle$ extrapolated to infinited total gas pressures (as mentioned in the text) in both argon and nitrogen buffer gases.

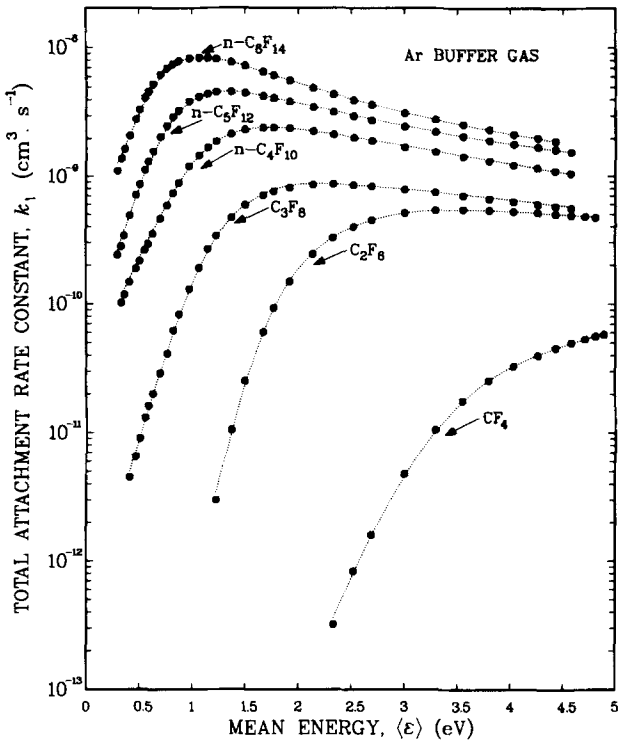

FIG. 9. Electron attachment rate constants k_1 for the perfluoroalkanes measured as a function of mean electron energy $\langle\epsilon\rangle$. The k_a ($\langle\epsilon\rangle$) for C_3F_8, n-C_4F_{10}, and n-C_5F_{12} are those extrapolated to infinite total gas pressures (measured in a buffer gas of argon).

TABLE II. Electron attachment rate constants for the perfluoroalkanes n-C_NF_{2N+2} ($N = 3$–6) in a buffer gas of N_2 as a function of E/N and $\langle\epsilon\rangle$.

			k_1($cm^3\ s^{-1}$)			
E/N (10^{-17} V cm^2)	$\langle\epsilon\rangle$ (eV)	w (10^5 cm s^{-1})	C_3F_8 (10^{-10})	n-C_4F_{10} (10^{-10})	n-C_5F_{12} (10^{-9})	n-C_6F_{14} (10^{-9})
0.0310	0.0404	1.10	0.016	0.41		0.23
0.0466	0.0430	1.53	0.018	0.41		0.23
0.0621	0.0463	1.87	0.019	0.41		0.24
0.0931	0.0546	2.33	0.019	0.41		0.24
0.124	0.0646	2.60	0.018	0.42		0.26
0.155	0.0757	2.73	0.019	0.43		0.26
0.186	0.0873	2.83	0.018	0.44		0.28
0.217	0.099	2.89	0.018	0.46		0.30
0.248	0.111	2.95	0.019	0.47		0.31
0.310	0.133	3.08	0.018	0.50		0.36
0.373	0.154	3.20	0.018	0.53		0.41
0.457	0.184	3.42	0.017	0.58	0.19	0.51
0.528	0.203	3.56	0.018	0.61	0.20	0.59
0.621	0.231	3.77	0.017	0.66	0.23	0.72
0.776	0.279	4.10	0.019	0.76	0.28	1.02
0.931	0.327	4.40	0.021	0.90	0.39	1.40
1.087	0.374	4.69	0.024	1.09	0.52	1.86
1.24	0.417	4.97	0.032	1.32	0.67	2.35
1.55	0.493	5.51	0.055	1.93	1.03	3.32
1.86	0.555	6.05	0.087	2.7	1.38	4.2
2.17	0.601	6.61	0.13	3.4	1.68	4.9
2.48	0.647	7.10	0.18	4.1	1.98	5.5
3.10	0.711	8.11	0.28	5.3	2.41	6.3
3.73	0.759	9.10	0.38	6.3	2.74	6.8
4.66	0.812	10.44	0.49	7.4	3.04	7.1
5.28	0.839	11.3	0.58	7.9	3.18	7.2
6.21	0.872	12.7	0.72	8.7	3.35	7.3
7.76	0.911	14.9	0.84	9.4	3.52	7.4
9.31	0.938	17.0	1.0	10.0	3.62	7.5
10.87	0.957	19.1	1.06	10.1	3.68	

TABLE III. Electron attachment rate constants for the perfluoroalkanes n-C_NF_{2N+2} ($N = 1$–6) in a buffer gas of argon as a function of E/N and $\langle\epsilon\rangle$.

			k_1(cm^3 s^{-1})					
E/N (10^{-18} V cm^2)	$\langle\epsilon\rangle$ (eV)	w (10^5 cm s^{-1})	CF_4 (10^{-11})	C_2F_6 (10^{-10})	C_3F_8 (10^{-10})	n-C_4F_{10} (10^{-9})	n-C_5F_{12} (10^{-9})	n-C_6F_{14} (10^{-9})
0.0932	0.300	0.903					0.24	1.10
0.124	0.335	0.963				0.102	0.28	1.38
0.155	0.364	1.013				0.118	0.34	1.65
0.217	0.412	1.097			0.045	0.148	0.49	2.10
0.311	0.473	1.200			0.065	0.188	0.71	2.83
0.373	0.509	1.258			0.09	0.216	0.86	3.35
0.466	0.559	1.335			0.13	0.262	1.12	4.1
0.528	0.590	1.38			0.16	0.293	1.31	4.6
0.621	0.634	1.44			0.20	0.352	1.58	5.3
0.777	0.702	1.53			0.29	0.46	2.06	6.2
0.932	0.764	1.61			0.41	0.59	2.50	6.9
1.09	0.822	1.68			0.62	0.74	2.94	7.5
1.24	0.876	1.75			0.83	0.89	3.30	7.9
1.55	0.976	1.87			1.30	1.20	3.88	8.3
1.86	1.068	1.95			1.90	1.47	4.2	8.4
2.17	1.15	2.03			2.66	1.70	4.5	8.4
2.49	1.23	2.10		0.030	3.38	1.90	4.6	8.2
3.11	1.37	2.22		0.105	4.7	2.17	4.6	7.8
3.73	1.50	2.33		0.252	5.9	2.34	4.5	7.3
4.66	1.67	2.46		0.61	7.0	2.43	4.3	6.6
5.28	1.77	2.54		0.93	7.6	2.43	4.2	6.2
6.21	1.92	2.64		1.48	8.1	2.40	3.91	5.6
7.77	2.14	2.79		2.42	8.5	2.28	3.53	5.0
9.32	2.33	2.92	0.032	3.25	8.6	2.15	3.24	4.4
10.97	2.52	3.04	0.083	3.96	8.5	2.03	3.00	4.0
12.4	2.69	3.14	0.16	4.46	8.3	1.92	2.78	3.69
15.5	3.00	3.33	0.48	5.11	7.9	1.71	2.49	3.18
18.6	3.29	3.49	1.05	5.38	7.5	1.56	2.26	2.83
21.7	3.55	3.63	1.76	5.43	7.0	1.43	2.08	2.58
24.9	3.80	3.76	2.53	5.37	6.6	1.32	1.92	2.35
27.9	4.03	3.88	3.28	5.25	6.3	1.22	1.80	2.15
31.1	4.26	3.99	3.97	5.14	6.0	1.16	1.70	2.00
34.2	4.43	4.18	4.54	5.01	5.8	1.10	1.63	1.90
37.3	4.58	4.38	5.00	4.90	5.6	1.05	1.56	
40.4	4.71	4.62	5.35	4.80				
43.5	4.81	4.90	5.62	4.70				
46.6	4.89	5.21	5.80					

expression[19]:

$$\tau_{att} = \frac{1}{\nu_{att}} = \int_0^\infty t\,(dn_e/dt)dt \Big/ \int_0^\infty \frac{dn_e}{dt}\,dt$$
$$= (\nu_2 + \nu_3)/\nu_1\nu_3.$$

Consequently,

$$\frac{1}{k_a} = \frac{1}{k_1} + \frac{\nu_2}{k_1 k_3 N_T}. \tag{9}$$

Thus, plotting the inverse of k_a as a function of the inverse of N_T allows k_1 to be determined from the intercept, while the slope yields ν_2/k_1k_3 from which the ratio ν_2/k_3 may be obtained. The ratio ν_2/k_3 is called the critical number density N_c,[20] where the rate of autoionization of the excited negative ion is equal to the rate of the collisional stabilization. Examples of the fit to this expression for C_3F_8 and n-C_4F_{10} in Ar are shown in Figs. 7(a) and 7(b), respectively. This expression is seen to give a good fit to the experimental data and has been found also to model the experimental attachment rate constants using N_2 as a buffer gas. Values of k_1 obtained in this manner for C_3F_8, n-C_4F_{10}, and n-C_5F_{12} in argon are given by the dashed lines in Figs. 4, 5, and 6, respectively. The values of k_1 obtained in the buffer gases N_2 and Ar are summarized in Figs. 8 and 9 and Tables II and III, respectively. These measurements indicate that as the size of the molecule increases from CF_4 to n-C_6F_{14}, the rate of electron attachment increases, the thresholds and peaks in the attachment rate constants vs $\langle\epsilon\rangle$ plots shift to lower energies, and the total pressure dependence of k_a decreases, such that for n-C_6F_{14} no pressure dependence is observed, even at the lowest pressures used in these experiments.

Several studies of the electron attachment coefficient η/N_a in *pure* CF_4 (Refs. 21–26), C_2F_6 (Refs. 21–24), C_3F_8 (Refs. 21, 24 and 27), n-C_4F_{10} (Refs. 21, 24, and 28), and n-C_6F_{14} (Ref. 21) have been made, but these measurements cannot be directly compared with the present results as the mean electron energies as a function of E/N are unknown for these gases. Pressure dependent electron attachment coefficients were observed for C_3F_8 (Refs. 24 and 27) and n-C_4F_{10}

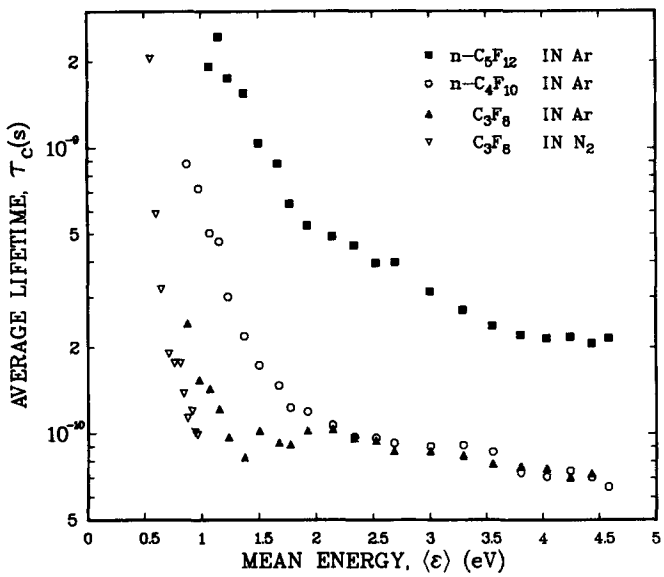

FIG. 10. The apparent lower limits to the lifetime τ_c of the excited transient parent negative ion of C_3F_8, n-C_4F_{10}, and n-C_5F_{12} as a function of the mean electron energy $\langle\epsilon\rangle$ in argon and nitrogen. At the low mean energies ($\langle\epsilon\rangle < 0.8$ eV) the lifetime of the excited transient parent anion is too long to be accurately calculated from the experimental measurements.

(Refs. 21, 24, and 28) in these studies but absent for CF_4 and C_2F_6, in agreement with the present study.

The average collision frequency ν_c between PFA^{-*} and M at N_c is given by $\nu_c = \langle v\rangle \sigma_L N_c$, where $\langle v\rangle$ is the average relative velocity between PFA^{-*} and M, and σ_L is the Langevin classical collision cross section, which for spiraling collisions at thermal energies is[29]

$$\sigma_L = \frac{2\pi}{\langle v\rangle}\left(\frac{e^2\alpha}{M_R}\right)^{1/2}, \tag{10}$$

where α is the static polarizability of M, e is the electronic charge, and M_R is the reduced mass of PFA^{-*} and M. The average lifetime between stabilizing collisions is

$$\tau_c = \tau_a/p = \frac{1}{\nu_c p} = \frac{1}{2\pi N_c p}\left(\frac{M_R}{e^2\alpha}\right)^{1/2}, \tag{11}$$

where $p \leqslant 1$ is the probability of stabilization at each PFA^{-*}–M collision and can vary considerably, depending on the relative velocity and nature of the PFA^{-*}–M pair.

Average lifetimes of the excited parent negative ion against autodetachment for C_3F_8, n-C_4F_{10}, and n-C_5F_{12} in Ar and C_3F_8 in N_2 have been calculated using Eq. (11) and are plotted in Fig. 10 as a function of mean electron energy. The differences between the calculated lifetimes for $C_3F_8^{-*}$ in N_2 and Ar in the region of overlap are thought to be due to the different probabilities of collisional stabilization of the parent ion in each $C_3F_8^{-*}$/buffer gas molecule collision. These calculations have been performed assuming $p = 1$, and it is emphasized that this probability may be significantly less than one. As a consequence, the calculated lifetimes shown in Fig. 10 are *lower* limits on the actual lifetimes of the excited parent negative ions.

These results indicate that the lifetime of the parent negative ion increases with increasing size of the molecule and decreasing electron energy. It is expected that as the size of the perfluoroalkane molecule increases, the electron affinity, and hence, the attachment rate and lifetime of the parent negative ion will increase.[8,20] Naidu and Prasad[24] have also found that for CF_4 and C_2F_6 the electron attachment rate was independent of the gas pressure, strongly pressure dependent for C_3F_8, and less dependent on total gas pressure in n-C_4F_{10}, with the greatest pressure dependence occurring at the higher E/N (hence $\langle\epsilon\rangle$) values, in agreement with the present study. It is likely that for the first two members of this series, namely, CF_4 and C_2F_6, the electron affinity of the parent molecule is negative or close to zero. This is supported by the results of MacNeil and Thynne,[30] Harland and Thynne,[31] and Spyrou *et al.*[8] in single collision experiments where no parent negative ions were observed for CF_4, C_2F_6, and C_3F_8. In contrast, a weak long-lived ($\simeq 20$ μs) parent negative ion was observed for n-C_4F_{10} by Harland and Thynne[32] and Spyrou *et al.*[8] The negative ion spectra of n-C_5F_{12} and n-C_6F_{14} are dominated by the formation of the metastable parent negative ions at epithermal energies ($\simeq 0.6$ eV).[8] Although metastable parent negative ions have not been observed for C_3F_8, Lifshitz and Grajower[33] obtained evidence for the existence of short-lived negative ion states at $\simeq 2.0$ eV, using the SF_6/scavenger technique for detecting indirectly scattered thermal electrons.[34]

It should be emphasized that in the single collision studies of Spyrou *et al.*,[8] MacNeil and Thynne,[30] and Harland and Thynne[31,32] only metastable parent negative ions with lifetimes $\geqslant 1$ μs and their dissociatively attached stable negative ion fragments are detected. In the swarm studies reported in this paper, the lifetimes of $C_3F_8^{-*}$, n-$C_4F_{10}^{-*}$, and n-$C_5F_{12}^{-*}$ are far too short to allow detection of those ions by single collision techniques. Conversely, negative ions with lifetimes of the order of 10^{-8} s or greater in the swarm studies would give attachment results which appear to be independent of total gas pressure, as they are all stabilized in collisions with the buffer gas at the total gas pressures used in these experiments. The electron attachment rate constant measurements are independent of the total gas pressure at the lower mean electron energies ($\langle\epsilon\rangle \leqslant 0.8$ eV) for the gases C_3F_8, n-C_4F_{10}, and n-C_5F_{12} (Figs. 4–6) in the present studies. The lifetimes of the parent anions in this situation may be as large as those observed in the single collision study[8] at these energies. Consequently, the fragment ions observed for C_3F_8 to n-C_6F_{14} in the single collision studies constitute only a small fraction of the total number of negative ions produced in the electron-perfluoroalkane collisions reported in this paper.

IV. ELECTRON ATTACHMENT CROSS SECTIONS

A. Electron energy distribution functions

The electron energy distribution functions $f(\epsilon, E/N)$ used in these experiments are assumed to be those of the pure buffer gas and that the addition of vanishingly small quantities (typically one part in 10^5 to 10^8) of attaching gas does not perturb $f(\epsilon, E/N)$. This implies that the transport parameters, such as w and D_T/μ (ratio of the transverse diffusion coefficient to the electron mobility), are similarly unaltered by the addition of the attaching gas. If the electron scattering cross sections for each of the buffer gases are known, it is

then possible to calculate $f(\epsilon, E/N)$ over a range of E/N values using a numerical solution of the Boltzmann equation for each of the pure buffer gases. For these studies, we used a numerical method developed by Phelps and co-workers and described in detail by Luft[36] to obtain $f(\epsilon, E/N)$ in N_2 and Ar, which we have checked against other numerical solutions by Morgan[37] and Gibson[38] and obtained excellent agreement.

Pitchford and Phelps[39] have recently shown that the addition of a small fraction of a highly attaching gas to a buffer gas (1–100 ppm of SF_6 in N_2 in their calculations) can considerably modify the electron energy distribution function and hence the transport parameters of the buffer gas. In the present measurements, the concentration of the attaching gas was adjusted such that 10% or fewer of the electrons were lost from the swarm by attachment over the E/N range of interest, and thus the effect on the distribution function from this source is negligible.

The accuracy of the attachment cross section obtained by this unfolding procedure is ultimately dependent upon the accuracy of the scattering cross sections used to obtain the energy distribution functions in each of these buffer gases. The scattering cross sections that are needed to analyze the attachment data in the present experiments lie in the energy range of from 0 to 10 eV and are the total momentum transfer cross section σ_m and the cross section for any inelastic processes in this energy region. σ_m is difficult to measure, particularly at low energies, and is usually obtained from an analysis of the Boltzmann equation, where a trial cross section is used to obtain a set of electron swarm transport parameters, usually w and D_T/μ. These parameters are then compared with experimental values and σ_m adjusted until the calculated and experimental parameters agree to within a given error.

Milloy *et al.*[40] and Haddad and O'Malley[41] have recently calculated σ_m in Ar up to 4 eV using the transport data of Robertson[14] for w and Milloy and Crompton[42,43] for D_T/μ. This cross section, along with that calculated by Frost and Phelps[44] at higher electron energies, has been used in the present studies. The inclusion of a total inelastic cross section with a threshold at 11.5 eV calculated by Specht *et al.*[45] and an ionization cross section of Rapp and Englander-Golden[46] with a threshold of 15.7 eV altered the transport coefficients calculated at the upper E/N values ($E/N < 4.8\times10^{-17}$ V cm^2) by less than 1%, in agreement with a previous study by Milloy.[47] This is to be expected as indicated in Fig. 11, where a typical set of distribution functions calculated in the present study are shown. It can be seen that the distribution functions do not contain significant contributions above 10 eV. The agreement between the experimental w measurements of Roberston[14] and the present calculated results are typically better than 1%. The calculated mean electron energies $\langle\epsilon\rangle$ and experimental D_T/μ value of Milloy and Crompton[43] are similarly in excellent agreement in the region of overlap with the present calculations. The maximum difference between the experimental D_T/μ values and

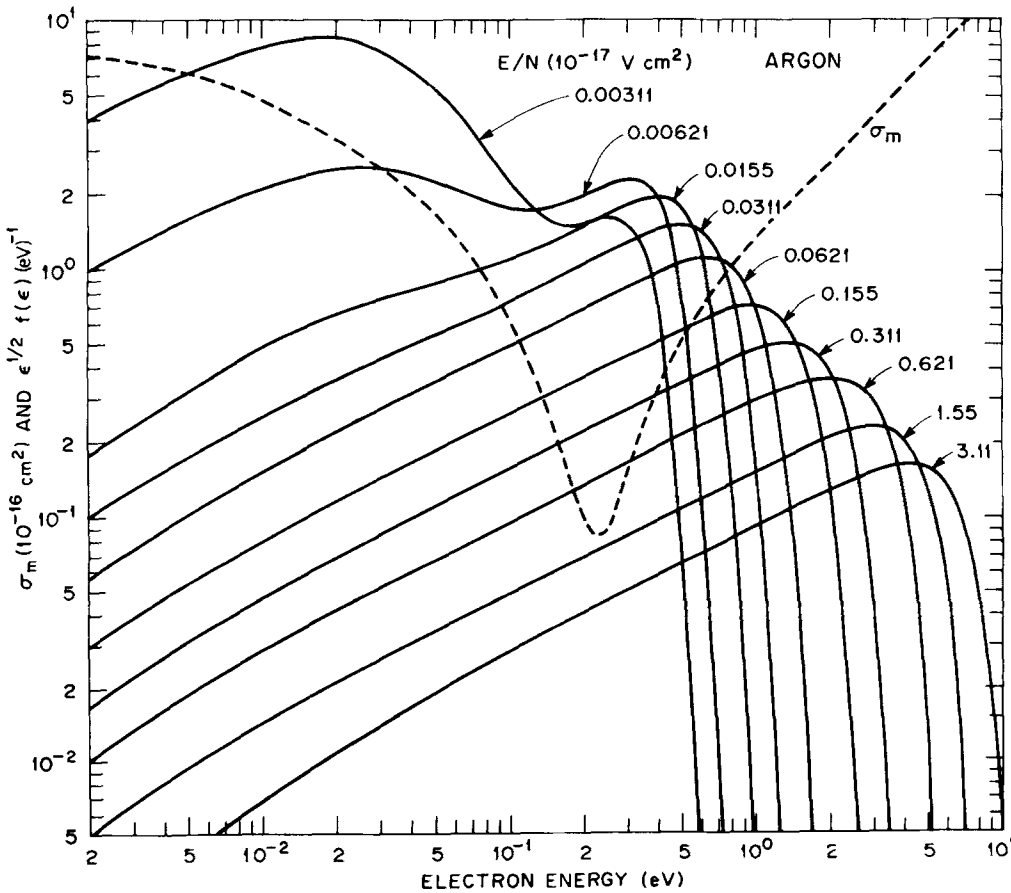

FIG. 11. Electron energy distribution functions for several E/N values in argon using the momentum transfer cross section σ_m of Milloy *et al.* (Ref. 40) and Haddad and O'Malley (Ref. 41).

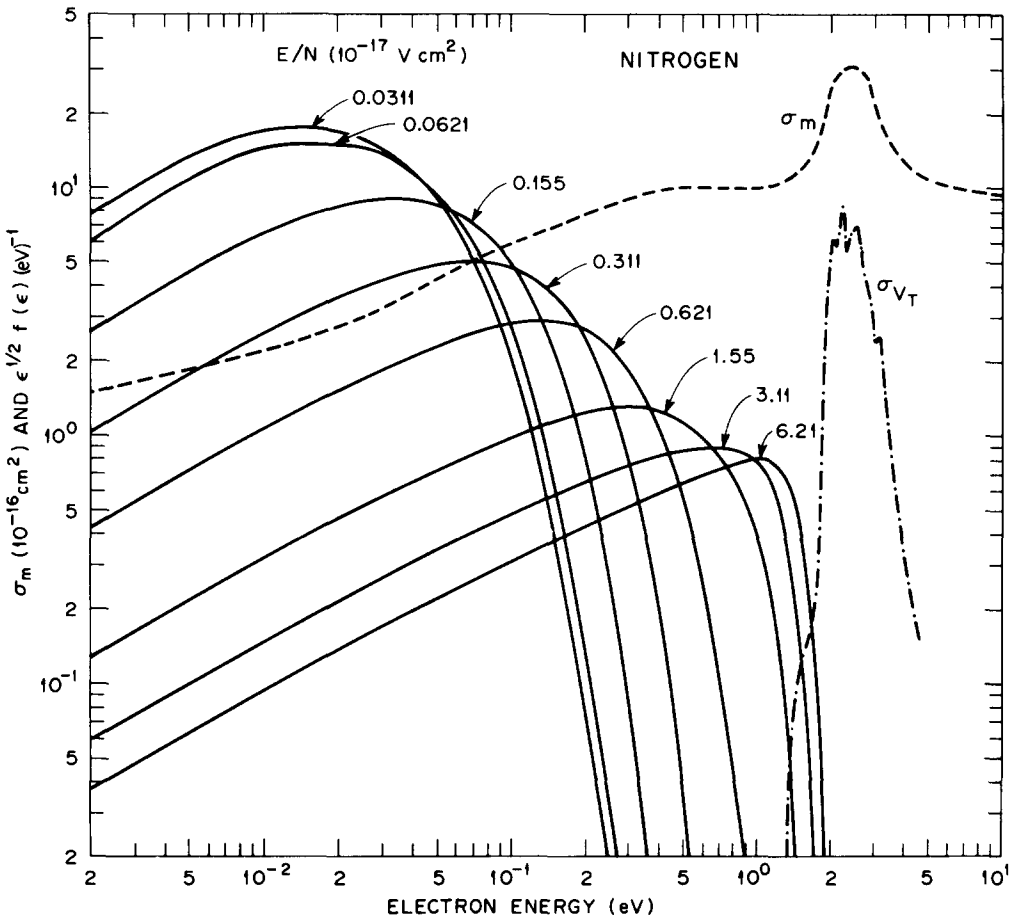

FIG. 12. Electron energy distribution functions for several E/N values in N_2 using the momentum transfer cross section σ_m of Phelps (Refs. 49 and 54) and the total vibrational excitation cross section σ_{V_T} of Schulz (Ref. 50) and Boness and Schulz (Ref. 51).

the present calculated values is 3%, which is similar to the difference that Milloy *et al.*[40] obtained between their experimental and calculated results.

A set of distribution functions in N_2 obtained in the present study are given in Fig. 12 along with the σ_m calculated by Engelhardt *et al.*[48] and Phelps[49] from an analysis of the transport data in N_2. Also included is the total vibrational cross section of Schulz[50] and Boness and Schulz[51] which was renormalized by Tachibana and Phelps[52] at energies above 1.6 eV. The agreement between the w values of Lowke[13] and Grünberg[16] and the D_T/μ values of Crompton and Elford[53] and the present calculated values is typically better than 5%. Phelps[54] has recently recalculated the vibrational cross sections in N_2, which now have somewhat different onsets and peak values, above 1.6 eV. As expected, this change has little influence on the derived transport data, except at the highest E/N values.

Considerable effort has been expended in recent years to probe the validity of the conventional solution of the Boltzmann equation, which involves a truncation after two terms (the so-called "two term approximation") of the distribution function expanded in a Legendre polynomial series.[55,66] This solution is expected to break down in situations where the electron scattering is highly anisotropic[58–60] or the ratio of inelastic collisions to elastic collisions is large.[58,61,62] The use of this approximation to calculate $f(\epsilon, E/N)$ in both N_2 and Ar has been questioned, primarily due to the depth of the minimum in σ_m in Ar[63] and the relatively large ratio of the sum of the vibrational states to σ_m in N_2.[64–66] These studies, using extended Boltzmann codes and Monte Carlo techniques, indicate that the two term approximation is valid in Ar and holds reasonably well in N_2 up to the maximum E/N ($\approx 2.0\times 10^{-16}$ V cm^2) in these experiments but begins to fail at higher E/N values. Although the use of the two-term Boltzmann equation to determine the electron energy distribution functions, and hence the electron attachment cross sections, becomes questionable at the highest E/N values in this study, Pitchford and Phelps[66] noted that the errors in the attachment cross sections derived in this manner should be small provided that the two-term derived scattering cross sections for N_2 are used with a two-term Boltzmann code to extract the attachment cross sections from the attachment rate constants.

Pitchford and Phelps[66] also noted a difference in the low-energy portion of the distribution functions between those calculated using the two- and multiterm Boltzmann codes and those obtained by the Monte Carlo technique developed by Reid.[58] If these differences were real, then it could have led to considerable differences in the attachment cross sections obtained using the two different distribution functions. Subsequent work[67] has established that there was an error in the scattering routine in Reid's[58] Monte Carlo code, which, when corrected, predicts distribution functions in agreement with those obtained by the Boltzmann analysis.

B. Swarm unfolded cross sections

The experimental attachment rate constants measured in the previous section were unfolded using an iterative swarm-unfolding technique originally devised by Christophorou *et al.*[35] to obtain the absolute total electron attachment cross section $\sigma_a(\epsilon)$ for each of the attaching molecules. The use of this unfolding procedure to generate attachment cross sections from the attachment rate constants requires a considerable degree of experience and discernment. The problem may be simply stated: At what point does one stop the iterating procedure and decide that the cross section that has been obtained represents the "true" or best approximation to the attachment cross section, free of the residual effects of the electron energy distribution function and the statistical uncertainties in the experimental data? Neither the distribution functions nor the data are completely free of error, and thus it is possible to apply the iterative procedure indefinitely and still not obtain an exact agreement between the calculated and experimental attachment rate constants.

In these experiments, the iterative procedure was continued until the percentage deviation between the calculated and experimental rate constants was $\leqslant 1.0\%$. Although the total estimated uncertainty in the experimental attachment rates is $\approx 5\%$–7% as shown in Table I, the statistical uncertainty in the data is considerably less, and thus it is justifiable to obtain a higher degree of agreement between the calculated and experimental rates [i.e., the shapes of the k_a $(\langle\epsilon\rangle)$ functions are more accurate than the overall magnitudes which are subject to errors in the pressure measurements, etc.]. In most cases, a percentage deviation of 1.0% is obtained within a few hundred iterations, and the resultant cross section is stable upon increasing the number of iterations. When the $k_a(\langle\epsilon\rangle)$ peaks at the last few E/N values or just beyond, as is the case for CF_4 (see Fig. 8), then considerably more iterations ($\geqslant 1000$) are required to obtain a stable solution, as the last few high-energy experimental data have a large influence on the final attachment cross section, even

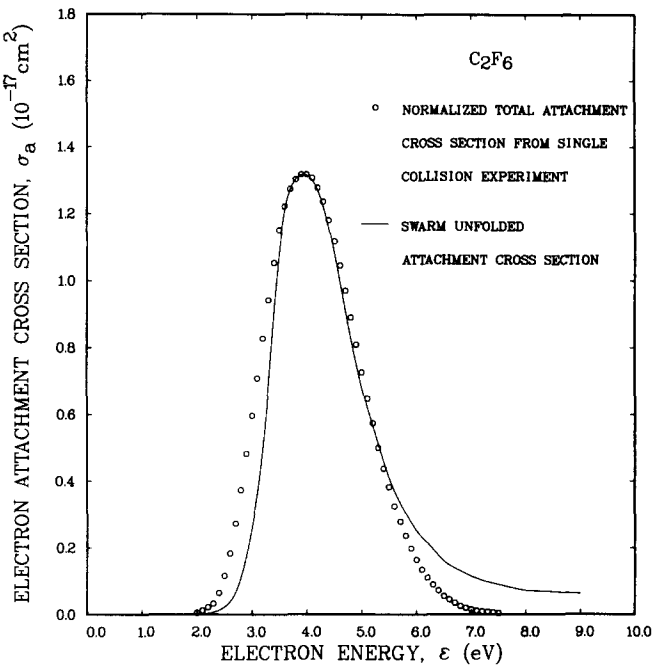

FIG. 14. Swarm unfolded total attachment cross section $\sigma_a(\epsilon)$ for C_2F_6 in comparison with the total relative negative ion cross section obtained in the single collision electron study of paper I (Ref.8).

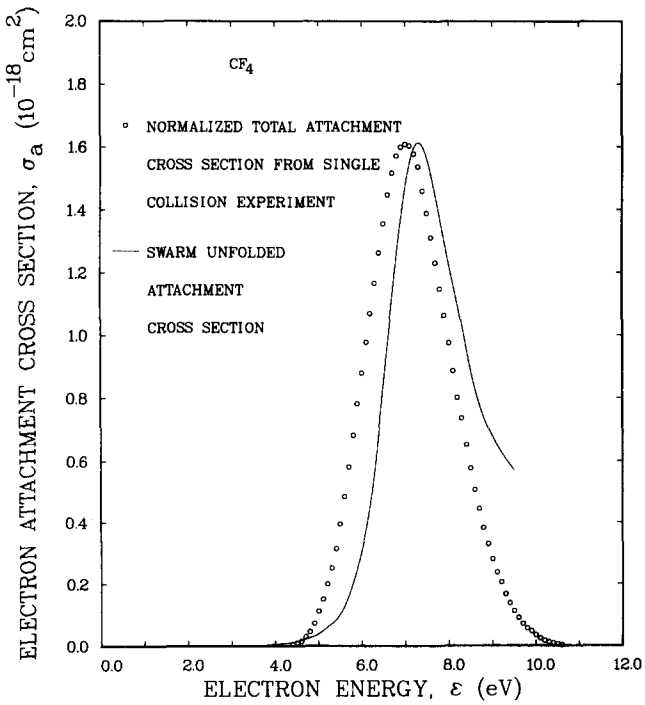

FIG. 13. Swarm unfolded total attachment cross section $\sigma_a(\epsilon)$ for CF_4 in comparison with the total negative ion yield obtained in the single collision electron beam study of paper I (Ref. 8). The beam relative cross section has been normalized to the peak in the unfolded cross section.

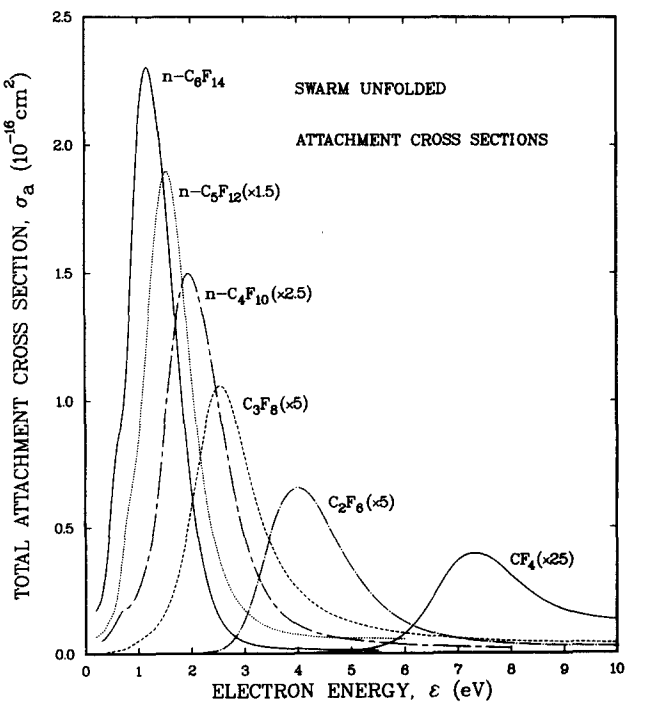

FIG. 15. The swarm unfolded total electron attachment cross section $\sigma_a(\epsilon)$ obtained from measurements of $k_a(\langle\epsilon\rangle)$ in Ar for the perfluoroalkanes n-C_NF_{2N+2} $(N = 1$–$6)$.

though the percentage deviation may have decreased to under 1.0% after a few hundred iterations.

The swarm unfolded $\sigma_a(\epsilon)$ for CF_4 is shown in Fig. 13 in comparison with the total negative ion yield obtained in paper I, which has been normalized at the peak to the present swarm unfolded $\sigma_a(\epsilon)$. The position of the peaks in the negative ion production cross sections and the half width of the resonance are in reasonable agreement. The position of the negative ion resonance in C_2F_6 obtained by the swarm unfolding and electron beam techniques is in considerably better agreement, although the agreement in the resonance half-width is poorer (see Fig. 14). It should be noted that in comparing the unfolded attachment cross sections obtained in the present experiments with the total negative ion yields obtained in paper I, it is assumed that the different negative ion species observed in that experiment are collected with the same efficiency. However, kinetic energy discrimination effects could possibly alter the collection efficiency for the various negative ion species, which when corrected, could lead to a closer agreement between the two sets of measurements. Comparison of the attachment cross sections obtained by these two techniques is not appropriate for the other perfluoroalkanes considered in this study. The cross sections obtained in the present study for these molecules are the effective cross sections for the production of the *initial* transient ($\tau_a < 10^{-8}$ s) parent negative ions, while the negative ion yields given in paper I are those for the production of long-lived ($\tau_a > 10^{-5}$ s) parent negative ions and negative ion fragments formed by dissociative attachment processes. The present calculated σ_a for the six perfluoroalkanes, obtained by unfolding the $k_a(\langle\epsilon\rangle)$ in argon, are given in Fig. 15 and are listed in Table IV. The estimated uncertainty in the magnitude, position, and half-width of the negative ion resonance cross sections for these molecules is less than $\pm$ 20%. The

TABLE IV. Electron attachment cross sections for the perfluoroalkanes n-C_NF_{2N+2} ($N = 1$–6) obtained by unfolding the electron attachment rate constants in argon.

	$\sigma_a(\epsilon)(\text{cm}^2)$					
ϵ (eV)	CF_4 (10^{-18})	C_2F_6 (10^{-17})	C_3F_8 (10^{-17})	n-C_4F_{10} (10^{-17})	n-C_5F_{12} (10^{-16})	n-C_6F_{14} (10^{-6})
0.20					0.045	0.172
0.25					0.050	0.193
0.30				0.209	0.054	0.214
0.35				0.235	0.062	0.281
0.40			0.012	0.285	0.078	0.362
0.5			0.019	0.40	0.102	0.61
0.6			0.027	0.55	0.155	0.83
0.7			0.036	0.67	0.264	0.94
0.8			0.051	0.74	0.372	1.18
0.9			0.077	0.84	0.46	1.64
1.0			0.105	1.02	0.56	2.05
1.1			0.134	1.29	0.71	2.26
1.2			0.165	1.69	0.89	2.30
1.3			0.201	2.02	1.06	2.20
1.4			0.251	2.88	1.19	2.04
1.5			0.326	3.66	1.26	1.83
1.6			0.42	4.4	1.25	1.59
1.7			0.55	5.1	1.17	1.33
1.8			0.71	5.7	1.05	1.08
1.9			0.92	6.0	0.89	0.85
2.0			1.15	6.0	0.74	0.65
2.1			1.40	5.8	0.61	0.50
2.3		0.007	1.87	5.0	0.396	0.276
2.5		0.025	2.11	4.0	0.261	0.152
2.7		0.072	2.04	3.05	0.179	0.089
3.0		0.263	1.57	1.85	0.114	0.046
3.3		0.66	1.10	1.13	0.080	0.029
3.6	0.001	1.09	0.77	0.72	0.062	0.022
4.0	0.004	1.32	0.51	0.45	0.049	0.018
4.5	0.014	1.08	0.335	0.287	0.042	0.014
5.0	0.039	0.69	0.247	0.215	0.040	0.012
5.5	0.102	0.41	0.194	0.170	0.039	0.011
6.0	0.31	0.250	0.159	0.139	0.037	
6.5	0.84	0.163	0.135	0.116	0.033	
7.0	1.47	0.115	0.118	0.099	0.028	
7.5	1.56	0.089	0.105	0.086	0.024	
8.0	1.23	0.073	0.096	0.076	0.020	
8.5	0.89	0.064	0.090	0.068	0.017	
9.0	0.68	0.057	0.086	0.061	0.014	
9.5	0.57	0.053	0.082	0.055		
10.0	0.52	0.049	0.078	0.049		

leading and trailing edges of the cross sections (particularly the high energy tails) have considerably larger uncertainties which are difficult to quantify.

Numerous negative ion studies have been performed for these molecules,[8] but only in two of these have attempts been made to obtain absolute negative ion production cross sections. The present peak value for σ_a of 1.6×10^{-18} cm^2 for CF_4 compares favorably with the value of $\sim1\times10^{-18}$ cm^2 obtained by Harland and Franklin.[68] The present peak value for σ_a of 1.3×10^{-17} cm^2 for C_2F_6 lies between the value obtained by Harland and Franklin[68] ($\sim6\times10^{-18}$ cm^2) and Kurepa[69] ($\sim2.1\times10^{-17}$ cm^2). Similarly, the present peak value of σ_a for C_3F_8 (2.1×10^{-17} cm^2) is bracketed by that obtained by Harland and Franklin[68] (2.5×10^{-18} cm^2) and Kurepa[69] ($\sim2.4\times10^{-16}$ cm^2). The uncertainties in the absolute magnitude of the electron beam derived cross sections are large due to uncertainties in the measurement of the gas pressure, the ion detection sensitivity, etc. Further, the beam cross section measurements for C_3F_8 should lie below the present measurements as only dissociatively attached negative ion fragments were observed in those studies, whereas as the present cross section for C_3F_8 also includes a contribution from the production of the initial transient parent negative ions.

V. THERMAL ELECTRON ATTACHMENT RATE CONSTANTS

The position and value of the cross section maxima and the thermal electron attachment rate constants $(k_a)_{\text{therm}}$ for the perfluoroalkanes studied are summarized in Table V. The $(k_a)_{\text{therm}}$ have been obtained by extrapolating the $k_a(\langle\epsilon\rangle)$ measurements, obtained in N_2 and given in Fig. 3, from the lowest value at $\langle\epsilon\rangle = 0.0404$ eV to $\langle\epsilon\rangle = 0.038$ eV corresponding to a gas temperature of 300 K, which was the temperature at which these measurements were performed. All these molecules have electron attachment rate constants and, hence, attachment cross sections which peak at electron energies well in excess of thermal energy; the larger the molecule, the larger the peak value in the rate constant which occurs at lower energies. The thermal attachment rates are correspondingly larger as the size of the molecule increases. The $(k_a)_{\text{therm}}$ value listed for n-C_5F_{12} is an upper limit as the sample used in these studies was possibly contaminated with up to 5% of c-C_5F_{10} which has an attachment cross section which peaks at thermal energies.[8] The present technique is not capable of obtaining accurate values of $k_a(\langle\epsilon\rangle)$ when these are of the order of 10^{-13} cm^3 s^{-1} or less. The $(k_a)_{\text{therm}}$ values for CF_4 and C_2F_6 are less than this value and, consequently, only an upper limit can be quoted for their $(k_a)_{\text{therm}}$ values. The only previous $(k_a)_{\text{therm}}$ measurements for CF_4, C_2F_6, and C_3F_8 are those of Davis *et al.*[70] who were again only able to obtain upper limits to the thermal attachment rates for these molecules. Their upper limit values are consistent with the present measurements.

VI. DISCUSSION AND CONCLUSIONS

A. Electron attachment reaction mechanisms

We have measured the electron attachment rate constants for the perfluoroalkane series n-C_NF_{2N+2} ($N = 1$–6) over a wide mean electron energy ($\langle\epsilon\rangle \simeq 0.04$ to 4.9 eV) and total pressure ($P_T = 130$ kPa to 3.3 MPa) range at room temperature ($T \sim 300$ K). These molecules are all saturated (single bonded) linear chain perfluorocarbons, and the present measurements show that as the size of the molecule increases, the rate of electron attachment increases and the peak position in the attachment rate shifts to lower energy. The measurements of $k_a(\langle\epsilon\rangle)$ for CF_4 and C_2F_6 are independent of P_T, indicating—as do the electron beam studies[8]—that dissociative electron attachment processes are responsible for the electron attachment observed for these molecules. In contrast, measurements of $k_a(\langle\epsilon\rangle)$ for C_3F_8 are highly dependent on P_T and tend to saturate as P_T increases above ~1.5 MPa. Similar, though smaller, pressure dependences were observed for n-C_4F_{10} and n-C_5F_{12} and found to be virtually absent for n-C_6F_{14}. The observed pressure dependences of $k_a(\langle\epsilon\rangle)$ have been interpreted as three-body stabilization of the short-lived (5×10^{-11} s $< \tau_a < 10^{-8}$ s) transient parent negative ions. The lifetimes of these anions increase with increasing size of the molecule and decreasing electron energy. These measurements imply that the electron affini-

TABLE V. Electron attachment cross section maxima, values of $\sigma_a(\epsilon)$ at these maxima, thermal attachment rate constants, and limiting breakdown strengths of the perfluoroalkanes n-C_NF_{2N+2} ($N = 1$–6).

Perfluoroalkane molecule	Cross section peak: Position (eV)	Cross section peak: Value σ_a (cm^2)	Rate constant k_a (0.038 eV) (cm^3 s^{-1})	Limiting breakdown strength $(E/N)_{\text{lim}}$ (10^{-15} V cm^2)
CF_4	7.3	1.58×10^{-18}	$<1\times10^{-13}$	1.41[a]
C_2F_6	4.0	1.32×10^{-17}	$<1\times10^{-13}$	2.75[a]
C_3F_8	2.55	2.12×10^{-17}	1.8×10^{-12}	3.60[a]
n-C_4F_{10}	1.95	6.0×10^{-17}	4.0×10^{-11}	4.72[a]
n-C_5F_{12}	1.55	1.26×10^{-16}	$<1.5\times10^{-10}$	5.94[b]
n-C_6F_{14}	1.20	2.60×10^{-16}	2.3×10^{-10}	7.66[b]

[a] From Ref. 3, measured at 1 atm.
[b] From Ref. 4.

ties (EA) of CF_4 and C_2F_6 are negative, while that of C_3F_8 is slightly positive and that the EA of the parent molecule increases in magnitude as the size of the perfluoroalkane increases. These observations are consistent with the single collision electron beam study reported in paper I[8] where long-lived parent negative ions were reported for n-C_4F_{10} and the larger perfluoroalkanes.

The positions of the negative ion states were found to decrease in energy and their cross sections to increase in magnitude with increasing molecular size in the analysis of the results given in paper I in agreement with the present study. Comparison of the positions and half-widths of the negative ion yields for CF_4 and C_2F_6 reported in paper I enabled us to make estimates of the absolute accuracy of electron attachment cross sections obtained by the swarm unfolding procedure. Comparison of the positions of the negative ion states for the larger perfluoroalkanes found in the two experiments is not possible due to the different decay mechanisms and energy dependences of the parent negative ions formed for these molecules.

B. Practical implications of the electron attachment measurements

One of the most important applications for these molecules is as high voltage gaseous[3–5] and liquid[6] insulants. The higher members of this series of molecules have high electric field breakdown strengths ($E/N_{\rm lim}$) as shown by the measurements listed in Table V and can possibly be used in place of, or as components in, multicomponent mixtures with SF_6 (Ref. 3 and 71) in high voltage applications. The strong pressure dependence in the attachment rates for C_3F_8 and n-C_4F_{10}, and to a lesser extent in n-C_5F_{12}, led to the prediction that the $E/N_{\rm lim}$ value in these gases would be dependent on the total gas pressure.[72] Subsequent studies[5,73] have indeed found a marked pressure dependent $E/N_{\rm lim}$ in C_3F_8 and n-C_4F_{10}. No pressure dependent breakdown measurements have yet been performed in n-C_5F_{12}.

A further promising application for these molecules is in mixtures in diffuse-discharge opening switching applications.[2] A primary requirement of a gas for this particular application is that it possesses negligible electron attachment at thermal energies and large electron attachment peaking at energies well in excess of thermal (i.e., $\epsilon > 1$–2 eV) (Refs. 2 and 74). The smaller molecules in the present study (i.e., CF_4–n-C_4F_{10}) possess very desirable energy dependent attachment rates for this particular application. It appears that the first few members of this series may also possess a Ramsauer-Townsend-type minimum in their momentum transfer scattering cross section (σ_m), which combined with large inelastic losses due to vibrational and/or rotational excitation near the minimum in σ_m lead to a large low E/N electron drift velocity in these gases and in mixtures and Ar and CH_4 which also possess Ramsauer–Townsend-type minima in their σ_m (Ref. 2). At higher E/N values, these gases and gas mixtures possess a negative differential conductivity region in which the electron drift velocity decreases with increasing E/N. This feature is again very attractive for diffuse-discharge switching applications.[2,74]

ACKNOWLEDGMENTS

The authors wish to thank J. L. Adcock and I. Sauers for performing the GC and positive ion mass specroscopy on these gas samples. We also wish to thank S. Ghemati for performing some initial measurements on n-C_6F_{14} and R. Y. Pai and V. E. Anderson for programming assistance and helpful discussions.

[1] L. G. Christophorou, D. L. McCorkle, D. V. Maxey, and J. G. Carter, Nucl. Instrum. Meth. **163**, 141 (1979); L. G. Christophorou, D. V. Maxey, D. L. McCorkle, and J. G. Carter, *ibid.* **171**, 491 (1980); M. K. Kopp, K. H. Valentine, L. G. Christophorou, and J. G. Carter, *ibid.* **201**, 395 (1982).
[2] L. G. Christophorou, S. R. Hunter, J. G. Carter, and R. A. Mathis, Appl. Phys. Lett. **41**, 147 (1982); L. G. Christophorou, S. R. Hunter, J. G. Carter, S. M. Spyrou, and V. K. Lakdawala, Proceedings of the 4th International Pulsed Power Conference, Albuquerque, New Mexico, June 6–8, 1983, p. 702; J. G. Carter, S. R. Hunter, L. G. Christophorou, and V. K. Lakdawala, Proceedings of the 3rd International Swarm Seminar, Innsbruck, Austria, August 3–5, 1983, p.30; P. Bletzinger, Proceedings of the 4th International Pulsed Power Conference, Albuquerque, New Mexico, June 6–8, 1983, p.37.
[3] D. R. James, L. G. Christophorou, and R. A. Mathis, in *Gaseous Dielectrics II*, edited by L. G. Christophorou (Pergamon, New York, 1980), p. 115; R. E. Wootton, S. J. Dale, and N. J. Zimmerman, *ibid*, p. 137.
[4] J. C. Devins, IEEE Trans. Electr. Insul. **15**, 81 (1980).
[5] G. Biasiutti, in *Gaseous Dielectrics III*, edited by L. G. Christophorou (Pergamon, New York, 1982), p. 174.
[6] J. K. Nelson and R. J. Manterfield, Proc. IEE **124**, 586 (1977).
[7] W. Braker and A. L. Mossman, *Matheson Gas Data Book*, 5th ed. (Matheson Gas Products, East Rutherford, New Jersey, 1971).
[8] S. M. Spyrou, I. Sauers, and L. G. Christophorou, J. Chem. Phys. **78**, 7200 (1983).
[9] T. E. Bortner and G. S. Hurst, Health Phys. **1**, 39 (1958).
[10] L. G. Christophorou, *Atomic and Molecular Radiation Physics* (Wiley-Interscience, New York, 1971), Chap. 4.
[11] A. A. Christodoulides, L. G. Christophorou, R. Y. Pai, and C. M. Tung, J. Chem. Phys. **70**, 1156 (1979); R. Y. Pai, L. G. Christophorou, and A. A. Christodoulides, *ibid.* **70**, 1169 (1979); A. A. Christodoulides and L. G. Christophorou, Chem. Phys. Lett. **61**, 553 (1979); D. L. McCorkle, A. A. Christodoulides, L. G. Christophorou, and I. Szamrej, J. Chem. Phys. **72**, 4049 (1980); D. L. McCorkle, I. Szamrej, and L. G. Christophorou, *ibid.* **77**, 5542 (1982).
[12] J. E. Turner (private communication).
[13] J. J. Lowke, Aust. J. Phys. **16**, 115 (1963).
[14] A. G. Robertson, Aust. J. Phys. **30**, 39 (1977).
[15] For example, see discussion by S. R. Hunter and L. G. Christophorou, in *Electron–Molecule Interactions and Their Applications*, edited by L. G. Christophorou (Academic, New York, 1984), Chap. 3, Vol. 2.
[16] R. Grünberg, Z. Naturforsch, Teil A **23** 1994 (1968).
[17] A. Bartels, Phys. Lett. A **44**, 403 (1973).
[18] *American Institute of Physics Handbook*, edited by D. E. Gray (McGraw-Hill, New York, 1957), Sec. 4.
[19] R. Grünberg, Z. Naturforsch. Teil A **24**, 1039 (1969).
[20] L. G. Christophorou, Chem. Rev. **76**, 409 (1976); Environ. Health Perspect. **36**, 3 (1980).
[21] J. C. Devins and R. J. Wolff, Annual Report on the Conference on Electrical Insulation (National Academy of Sciences—National Research Council, Washington, D.C., 1964), p. 43.
[22] S. E. Bozin and C. C. Goodyear, Brit. J. Appl. Phys. (J. Phys. D) **1**, 327 (1968).
[23] I. M. Bortnik and A. A. Panov, Sov. Phys.-Tech. Phys. **16**, 571 (1971).
[24] M. S. Naidu and A. N. Prasad, J. Phys. D **5**, 983 (1972).
[25] C. S. Lakshminarasimha, J. Lucas, and D. A. Price, Proc. IEE **120**, 1044 (1973); C. S. Lakshminarasimha, J. Lucas, and R. A. Snelson, *ibid.* **122**, 1162 (1975).
[26] M. Shimozuma, H. Tagashira, and H. Hasegawa, J. Phys. D **16**, 971 (1983).
[27] J. L. Moruzzi and J. D. Craggs, Proc. Phys. Soc. London **82**, 979 (1963).
[28] S. A. A. Razzak and C. C. Goodyear, Brit. J. Appl. Phys. (J. Phys. D) **1**, 1215 (1968).
[29] L. G. Christophorou, *Atomic and Molecular Radiation Physics* (Wiley-Interscience, New York, 1971), Chap. 7.

[30]K. A. G. MacNeil and J. C. J. Thynne, Int. J. Mass Spectrom. Ion Phys. **2**, 1 (1969); **3**, 455 (1970).
[31]P. W. Harland and J. C. J. Thynne, Int. J. Mass. Spectrom. Ion Phys. **9**, 253 (1972).
[32]P. W. Harland and J. C. J. Thynne, Int. J. Mass. Spectrom. Ion Phys. **11**, 445 (1973).
[33]C. Lifshitz and R. Grajower, Int. J. Mass. Spectrom. Ion Phys. **4**, 92 (1970).
[34]R. K. Curran, J. Chem. Phys. **38**, 780 (1963).
[35]L. G. Christophorou, D. L. McCorkle, and V. E. Anderson, J. Phys. B **4**, 1163 (1971).
[36]P. E. Luft, JILA Information Center Report No. 14, Boulder, Colorado (1975).
[37]W. L. Morgan, JILA Information Center Report No. 19, Boulder, Colorado (1979).
[38]D. K. Gibson, Aust. J. Phys. **23**, 683 (1970) and M. T. Elford (private communication, 1982).
[39]L. C. Pitchford and A. V. Phelps, Bull. Am. Phys. Soc. **28**, 182 (1983).
[40]H. B. Milloy, R., W. Crompton, J. A. Rees, and A. G. Robertson, Aust. J. Phys. **30**, 61 (1977).
[41]G. N. Haddad and T. F. O'Malley, Aust. J. Phys. **35**, 35 (1982).
[42]H. B. Milloy and R. W. Crompton, Aust. J. Phys. **30**, 51 (1977).
[43]H. B. Milloy and R. W. Crompton, Aust. J. Phys. **35**, Corrigendum-105 (1982).
[44]L. S. Frost and A. V. Phelps, Phys. Rev. A **136**, 1538 (1964).
[45]L. T. Specht, S. A. Lawton, and T. A. DeTemple, J. Appl. Phys. **51**, 166 (1980).
[46]D. Rapp and P. Englander-Golden, J. Chem. Phys. **43**, 1464 (1965).
[47]H. B. Milloy, J. Phys. B **8**, L414 (1975).
[48]A. G. Engelhardt, A. V. Phelps, and C. G. Risk, Phys. Rev. A **135**, 1566 (1964).
[49]A. V. Phelps (private communication, 1978) and Thirty-First Gaseous Electronics Conference, Buffalo, New York, October 17–20, 1978.
[50]G. J. Schulz, Phys. Rev. **135**, 988 (1964).
[51]M. J. W. Boness and G. J. Schulz, Phys. Rev. A **8** 2883 (1973).
[52]K. Tachibana and A. V. Phelps, J. Chem. Phys. **71**, 3544 (1979).
[53]R. W. Crompton and M. T. Elford, Electron and Ion Diffusion Unit, Australian National University, Quarterly Report **19** (1965).
[54]A. V. Phelps (private communication, 1982).
[55]For a recent review of the numerical techniques that have been used to probe the validity of the assumptions inherent in the solution of the Boltzmann transport equation, see S. R. Hunter and L. G. Christophorou, in *Electron–Molecular Interactions and Their Applications*, edited by L. G. Christophorou (Academic, New York, 1984), Chap. 3, Vol. 2.
[56]L. Ferrari, Physica A **81**, 276 (1975); L. Ferrari, Physica C **85**, 161 (1977).
[57]P. Kleban and H. T. Davis, Phys. Rev. Lett. **39**, 456 (1977); J. Chem. Phys. **68**, 2999 (1978); P. Kleban, L. Foreman, and H. T. Davis, *ibid.* **73**, 519 (1980).
[58]I. D. Reid, Aust. J. Phys. **32**, 231 (1979).
[59]I. D. Reid and S. R. Hunter, Aust. J. Phys. **32**, 255 (1979).
[60]G. N. Haddad, S. L. Lin, and R. E. Robson, Aust. J. Phys. **34**, 243 (1981).
[61]S. L. Lin, R. E. Robson, and E. A. Mason, J. Chem. Phys. **71**, 3483 (1979).
[62]G. N. Haddad and M. T. Elford, J. Phys. B **12**, L743 (1979).
[63]H. B. Milloy and R. O. Watts, Aust. J. Phys. **30**, 73 (1977); G. L. Braglia and A. Baiocchi, Physica C **95**, 227 (1978); G. N. Haddad and R. W. Crompton, Aust. J. Phys. **33**, 975 (1980); T. Makabe and T. Mori, J. Phys. D **15**, 1395 (1982).
[64]G. L. Braglia, R. Bruzzese, S. Solimeno, S. Martelluci, and J. Quartieri, Lett. Nuovo Cimento **30**, 459 (1981); G. L. Braglia, L. Romano, and M. Diligenti, *ibid.* **35**, 193 (1982); Phys. Rev. A **26**, 3689 (1982).
[65]L. C. Pitchford, S. V. O Neil, and J. R. Rumble, Jr., Phys. Rev. A **23**, 294 (1981).
[66]L. C. Pitchford and A. V. Phelps, Phys. Rev. A **25**, 540 (1982).
[67]I. D. Reid and L. C. Pitchford (private communications, 1982) and R. W. Crompton and G. N. Haddad, Ion Diffusion Unit, Australian National University Quarterly Report **85**, 5 (1981). I. D. Reid, Aust. J. Phys. **35**, Corrigendum-473 (1982).
[68]P. W. Harland and J. L. Franklin, J. Chem. Phys. **61**, 1621 (1974).
[69]M. V. Kurepa, 3rd Czechoslavakian Conference on Electronics and Vacuum Physics Transactions (1965), p. 107.
[70]F. J. Davis, R. N. Compton, and D. R. Nelson, J. Chem. Phys. **59**, 2324 (1973).
[71]L. G. Christophorou, D. R. James, I. Sauers, M. O. Pace, R. Y. Pai, and A. Fatheddin, in *Gaseous Dielectrics III*, edited by L. G. Christophorou (Pergamon, New York, 1982), p. 151.
[72]S. R. Hunter, L. G. Christophorou, D. R. James, and R. A. Mathis, in *Gaseous Dielectrics III*, edited by L. G. Christophorou (Pergamon, New York, 1982), p. 7.
[73]K. Nakanishi, D. R. James, H. Rodrigo, and L. G. Christophorou J. Phys. D (in press).
[74]R. F. Fernsler, D. Conte, and I. M. Vitkovitsky, IEEE Trans. Plasma Sci. **PS-8**, 176 (1980); K. H. Schoenbach, G. Schaefer, M. Kristiansen, L. L. Hatfield, and A. H. Guenther, IEEE Trans. Plasma Sci. **PS-10**, 246 (1982).